

Nitric-oxide photorelease and photoinduced linkage isomerism on solid [Ru(NO)(terpy)(L)]BPh₄ (L = glycolate dianion)[†]

Helene Giglmeier,^a Tobias Kerscher,^a Peter Klüfers,^{*a} Dominik Schaniel^b and Theo Woike^{*b}

Received 23rd June 2009, Accepted 28th August 2009

First published as an Advance Article on the web 7th September 2009

DOI: 10.1039/b912162e

Following photoexcitation at 80 K, two phenomena were detected on solid samples of a single substance, the tetraphenylborate of the [Ru(NO)(terpy)(L)]⁺ cation (terpy = 2,2′:6′,2′′-terpyridine, L = glycolate(2−) [oxycetate]): the formation of photoinduced linkage isomers of the nitrosyl ligand, and photorelease of nitric oxide. Populations of about 9% and 4% were measured for the photoinduced isonitrosyl (MS1) and the side-on nitrosyl (MS2) linkage isomers, respectively. At room temperature, NO release in the solid was observed as the only reaction.

The extensively studied photoreactivity of {RuNO}⁶-type nitrosyl complexes is dominated by two processes (*cf.* ref. 1 for the electron-counting rules of the Enemark–Feltham notation). The first is the photorelease of nitric oxide which is sometimes followed by the recombination of NO and the metal centre.² The second is the photoinduced formation of nitrosyl linkage isomers.^{3–5} For the linkage isomers, two forms that are energy-rich with respect to the κN-bonded nitrosyl ground-state (GS) have been detected for metal nitrosyls: the κO-bonded, isonitrosyl state (MS1), and the κN,O-bonded, side-on nitrosyl state (MS2). Though a relationship between both phenomena has been discussed,^{2,6} the individual experimental setups used for the detection of either phenomenon are different. Typically, a photorelease (PR) study is conducted close to the experimental boundary conditions of the attempted application, namely the medical usage of a, hopefully, switchable NO donor under physiological conditions. Accordingly, PR is investigated mostly in aqueous solution close to or above room temperature. As a result of these conditions, the final photoproducts are usually nitric oxide and the aquaruthenium(III) analogue of the nitrosyl starting complex. In contrast, photoinduced linkage isomerism (PLI) is detected mostly in the solid state and at substantially lower temperatures. However, recent studies show that the PLI phenomenon does not depend on the existence of a cavity inside a crystal but may be observed in solution as well.^{7,8} Conversely, PR may also occur in the solid state and has been considered a reason for the decrease of the achievable population of photoinduced linkage isomers on irradiation with light in the spectral range below 458 nm in the course of a typical PLI experiment on the pyridine (py) complex

trans-[RuCl(NO)(py)₄](PF₆)₂·½H₂O.⁹ It should be noted that in the case of solid-state PR, the nature of the photoproducts is expected to be convoluted. Motivated by the observation that PR may interfere with PLI in a solid, we started a more systematic search for substances that show both PLI and PR and thus allow the study of the connection or competition between both excitation paths in more detail. As a result, we are presenting a preliminary study on a terpyridine-glycolate(2−)-coordinated {RuNO}⁶-type cation whose tetraphenylborate salt reacted on irradiation with the formation of two photoinduced isomers as well as with nitric-oxide release.[‡]

The title compound was prepared by the reaction of [Ru(NO)(terpy)Cl₂]PF₆ with excess glycolic acid and slightly more than an equimolar amount of sodium hydroxide to achieve deprotonation of both the carboxylic and the hydroxy function to a dianionic glycolate(2−) ligand. In agreement with the strong π acidity of the nitrosyl ligand, the substitution reaction yielded the product with the alkoxide function of the glycolate(2−) ligand *trans* to NO and the carboxylate in the terpy plane. Crystals of the dmsolvate of the tetraphenylborate of the nitrosyl-ruthenium cation were obtained by the addition of sodium tetraphenylborate to the aqueous reaction mixture and recrystallisation from dmsolvate. The crystal-structure analysis of this [Ru(NO)(terpy)L]BPh₄·dmsolvate (1·dmsolvate) showed disordered dmsolvate molecules close to the nitrosyl ligand. The [Ru(NO)(terpy)L]⁺ ions in crystals of 1·dmsolvate exhibit non-crystallographic C_s symmetry (Fig. 1). The apparent octahedral coordination of the central metal is distorted from its ideal position in two respects. First, the N–Ru–N angle in the molecular mirror plane (N2–Ru1–N4 in Fig. 1) is about 10°

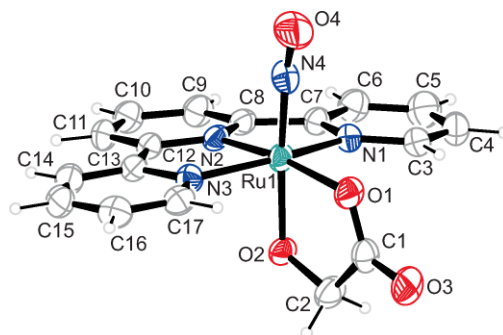


Fig. 1 The molecular structure of the cations of **1** in crystals of the tetraphenylborate's dmsolvate (50% probability ellipsoids). Distances (Å) and angles (°): from Ru1 to: N4 1.750(4), O2 1.939(2), N2 1.977(3), O1 2.039(2), N1 2.082(3), N3 2.088(3); O4–N4 1.157(4); O4–N4–Ru1 167.1(3), N4–Ru1–N2 99.2(1), N4–Ru1–O1 89.8(1), N4–Ru1–O2 172.3(1); chelate torsion: O2–C2–C1–O1 −3.1(5), N2–C12–C13–N3 −2.0(5), N1–C7–C8–N2 1.4(5).

^aDepartment für Chemie und Biochemie, Ludwig-Maximilians-Universität, Butenandtstraße 5–13, 81377 München, Germany. E-mail: kluef@cup.uni-muenchen.de; Fax: +89218077407; Tel: +89218077404

^bI. Physikalisches Institut, Universität zu Köln, Zùlpicherstraße 77, 50937 Köln, Germany. E-mail: th.woike@uni-koeln.de; Fax: +2214705162; Tel: +2214706355

[†]CCDC reference number 736561. For crystallographic data in CIF or other electronic format see DOI: 10.1039/b912162e

larger than a right angle. Second, the nitrosyl-O atom is tilted another 10° , in the mirror plane, towards the carboxylato ligand. In agreement with its embedding in the “soft” tetraphenylborate counterions and disordered dmsolvent molecules, these tilts are not caused by packing forces. In fact, the molecular parameters of the cation are well reproduced by means of a DFT calculation on the cation in vacuum. Also in agreement with this finding is the structure of the related $[\text{Ru}(\text{NO})(\text{terpy})(\text{OH})\text{Cl}]^+$ ion in crystals of the solvent-free hexafluoridophosphate, which shows essentially the same direction and amount of distortion.¹⁰

Both metastable states, MS1 and MS2, were generated in **1** by illumination in the blue-green spectral range at $T = 80$ K. Illumination in the spectral range of 532–442 nm resulted in the generation of MS1 with a maximal population of 9.5% at 488 nm. By subsequent irradiation of MS1 with $\lambda = 1064$ nm, about half of the MS1 isomer was transferred to MS2 resulting in a MS2 population of 4% (the other half returned to the GS). The identification of MS1 and MS2 was performed by infrared spectroscopy in the spectral range of the $\nu(\text{NO})$ stretching vibration. As can be seen from Fig. 2, the area of the GS band at 1861 cm^{-1} decreased upon illumination (488 nm) and a novel band at a lower energy of 1732 cm^{-1} (MS1) appeared. On continuing the illumination with 1064 nm, the MS1 band decreased and a second new band at 1550 cm^{-1} (MS2) appeared. At the same time, the GS band increased slightly. After a sufficiently long period of illumination with 1064 nm radiation, the MS1 and MS2 bands disappeared completely, while the GS band area was not completely restored (36% missing). Since MS1 and MS2 were completely erased, the missing area was attributed to nitric oxide release. The MS1 and MS2 populations as well as the amount of NO release were determined from the areas of the $\nu(\text{NO})$ vibrations. Since the MS1 population was saturated at 9.5% after the first irradiation step of $Q = 151\text{ J cm}^{-2}$, the further decrease of the GS band area during illumination with 488 nm was due to NO release as illustrated in

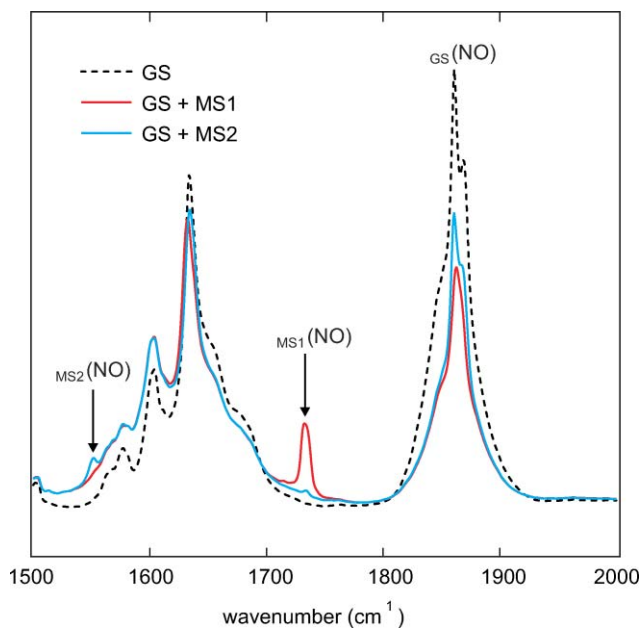


Fig. 2 IR spectra in the $\nu(\text{NO})$ range ($T = 80$ K). The MS1 isomer was populated by irradiation at 488 nm, and subsequently transferred to about equal parts of GS and MS2 by irradiation at 1064 nm.

Fig. 3. In order to investigate the release of nitric oxide without the disturbance by PLI, we investigated the NO release at room temperature where the lifetimes of MS1 and MS2 were too short to be observed. In Fig. 3 the reduction of the GS $\nu(\text{NO})$ band area during illumination with 442.5 nm radiation at $T = 294$ K is shown as a function of exposure $Q = \int I dt$ ($I =$ intensity). Both NO-release kinetics at low and room temperature needed to be described with a sum of two exponentials (Fig. 3). The values given in Fig. 3 show that NO release is faster and more efficient at higher temperature and higher illumination energy.

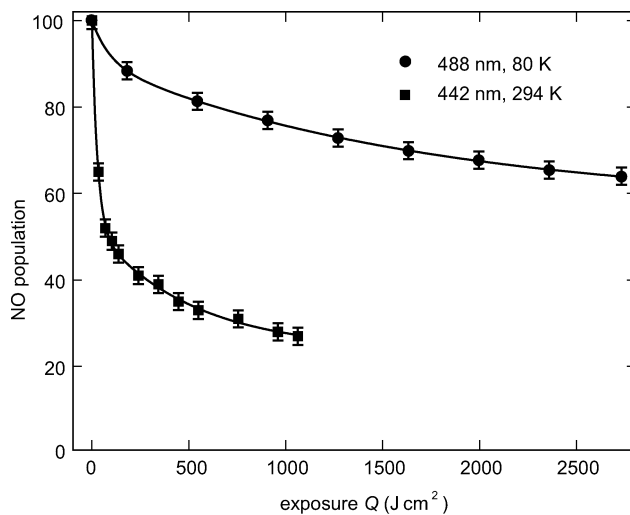


Fig. 3 NO release on irradiation with 442.5 nm light at room temperature ($T = 294$ K) and with 488 nm light at $T = 80$ K over the total exposure Q . The NO population is given as the area of the $\nu(\text{NO})$ stretch. The observed data were fitted by: $\text{NO population} = y_0 + A_1 \exp(-Q/Q_1) + A_2 \exp(-Q/Q_2)$ with y_0 being the offset at $Q = \infty$, the amplitudes $A_{1,2}$ and the $Q_{1,2}$ values which corresponds to a curve's decline to e^{-1} . The low-temperature fit results were: $y_0 = 57.3(9)\%$, $A_1 = 33.1(5)$, $Q_1 = 1700(100)\text{ J cm}^{-2}$; $A_2 = 9.5(5)$, $Q_2 = 91(10)\text{ J cm}^{-2}$. The room-temperature values were: $y_0 = 24(2)\%$, $A_1 = 28(2)$, $Q_1 = 500(60)\text{ J cm}^{-2}$; $A_2 = 48(2)$, $Q_2 = 28(2)\text{ J cm}^{-2}$.

The spectral range for PLI and PR is identical for **1**. The charge-transfer transition $\text{Ru}(4d) \rightarrow \pi^*(\text{NO})$ seems to induce both processes. Hence, in light of the excitation paths discussed in ref. 11 we have two possible scenarios: first, a one-step process in which after the excitation to the $\pi^*(\text{NO})$ the NO ligand relaxes either into MS2 by rotation of roughly 90° or the NO ligand is released. Second, a two-step process in which first MS2 is reached (rotation of NO by about 90° , ≈ 1 eV above GS) from where, with a second excitation at the same wavelength, NO release occurs. The release *via* occupation of the MS1 state is very improbable since, up to now, the existence of MS1 at room temperature could not be verified using short laser pulses for excitation.⁷ At low temperature PLI competes with PR. The population and transfer characteristics of PLI in **1** show that it behaves as in other PLI compounds and can thus be explained within the above-mentioned generalised potential scheme.¹¹ PR at low temperature might thus occur as discussed above or *via* MS1.

The characteristics of the bonding situation were evaluated in a preliminary DFT study on the GS of the cation of **1**, some linkage isomers, and the *trans*-carboxylato isomer. The latter isomer was not expected in light of the *trans*-to-NO-ligand specificity formulated above. In fact, the *trans*-carboxylato isomer that bears

Table 1 Computational results for the GS, three MS2, the MS1 and the carboxylate-alkoxide-converted *trans*-carboxylate isomer. In the C_1 -symm. MS2, the NO ligand is about perpendicular to the complex ion's mirror plane. The other states are depicted in Fig. 4. For the scaling factor applied to calculated frequencies see ref. 21

	GS	MS2 _{min}	MS2 _{max}	C_1 -symm. MS2	MS1	<i>trans</i> -COO
$E/\text{kJ mol}^{-1}$	0	116	140	122	174	14
E/eV	0	1.20	1.45	1.27	1.81	0.15
$0.961 \times \nu(\text{NO})_{\text{calc}}$	1863	1578	1579	1587	1807	1867
$\nu(\text{NO})_{\text{exp}}$	1861	1550	1734			

the less π -donating group *trans* to the π -accepting nitrosyl ligand is less stable, but moderately so, on the chosen level of theory (Table 1). The calculation, the results of which are collected in Table 1, predicted energetic and vibrational parameters. For the NO stretch, experimental and calculated values reasonably match for the GS and MS2 states. However, the experimental value for MS1 indicates a more pronounced softening of the NO stretch than predicted by the calculation. The methodological background of this generally observed but yet unmastered problem has been addressed in recent theoretical work.^{12,13}

In terms of bonding, the comparison of **1** and the $\{\text{RuNO}\}^6$ moiety in the related $[\text{Ru}(\text{NO})(\text{NH}_3)_5]^{2+}$ ion showed the influence of the glycolato(2-) ligand.^{4,14-17} Thus, the frontier orbitals of the

latter are Ru- and NO-centered whereas the ammine-centered orbitals are more stable and show no significant contributions to nitrosyl-ruthenium bonding. The same was found for the Ru-terpy interaction in this work. Specifically, Ru-NO bonding is characterised by the same types of interaction among the various stable and metastable isomers, namely an NO-to-Ru σ donor bond and two Ru-to-NO π back bonds. The bonding situation in the title cation resembles this latter picture. Fig. 4 shows, using the example of MO 92 which contributes to one of the two π back bonds, the largely unchanged shape of this orbital throughout the four minimum structures. (The depicted minima were reached along a full rotation of the nitrosyl ligand in the cation's apparent mirror plane. In addition, two symmetrically equivalent MS2 isomers

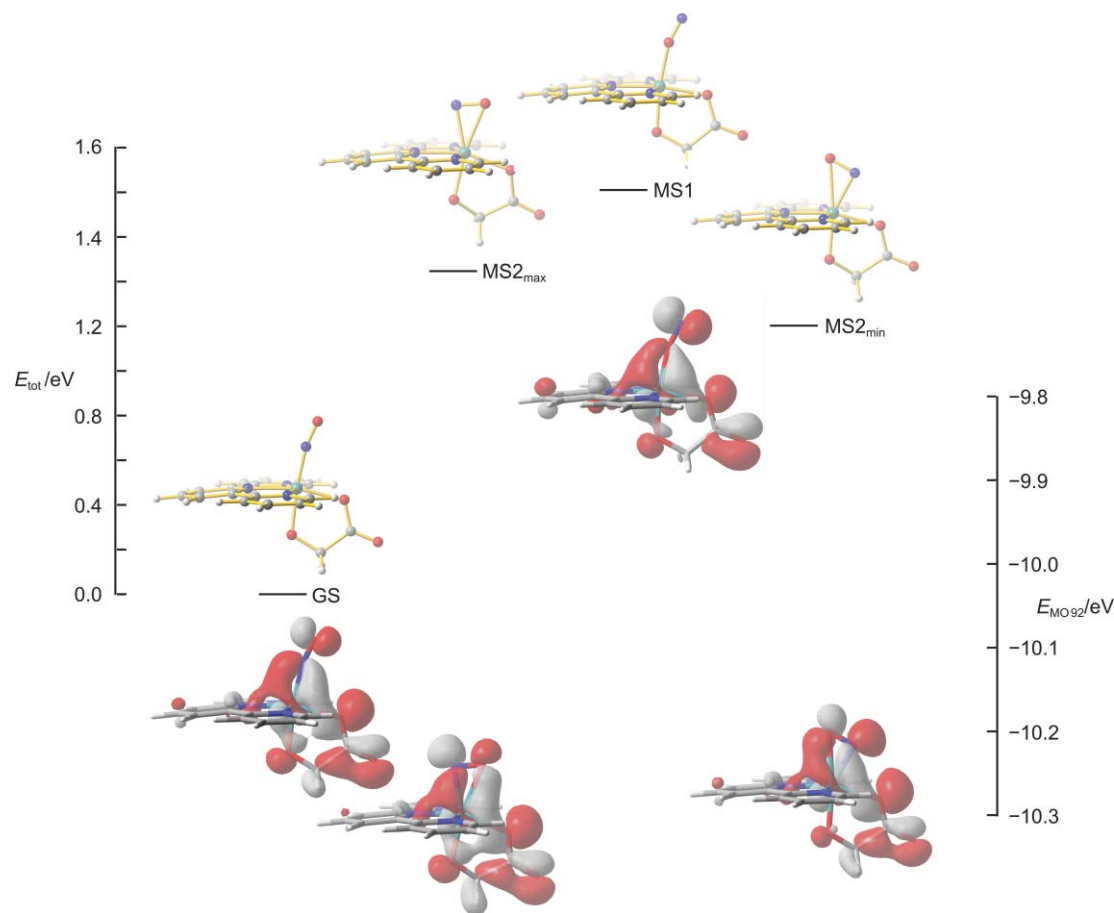


Fig. 4 Ball-and-stick drawings: the four minimum structures on the hypersurface of the electronic ground state which are reached, from the left to the right, by a clockwise rotation of the nitrosyl ligand in the mirror plane of the cation of **1**. The relative total energies (left scale, GS set to zero) refer to the bar at the respective isomer's label. Molecular orbital drawings: the occupied MOs (no. 92) which correspond mainly to the glycolate(2-)-assisted Ru(d_{yz})-to-NO(π^*) back bond (y to the right, z up). An orbital's energy may be roughly assessed from its position with respect to the right scale.

were found with the nitrosyl ligand perpendicular to the mirror plane.) The almost constant orbital shape is a common feature of the title cation and the ammine-nitrosyl complex. A marked difference, however, is the contribution of the dianionic ligand's atomic orbitals to the Ru–NO back bond and the other frontier orbitals. A bonding interaction between the anion and the formal NO⁺ species would, moreover, be a reason for the peculiar tilt of the nitrosyl towards the glycolate(2[−]) ligand in most of the states.

In conclusion, both significant excitation phenomena of a metal nitrosyl complex—photoinduced linkage isomerism and photorelease of nitric oxide—were observed on irradiation of solid samples of **1**. Remarkably, at a lower temperature, photorelease was observed in the same samples that showed PLI. The title compound thus appears to be a useful tool to investigate the connection of PLI and PR, which may be either consecutive or competing or non-related phenomena. The molecular structure of the nitrosyl complex, both experimental and calculated, points towards the usability of a hypothesis that is presently emerging from DFT calculations on related {RuNO}⁶⁻-type amino-acid complexes.¹⁸ These calculations show, formulated in a strongly simplified way, that the ligand *trans* to the Ru–NO axis contributes to the properties of the Ru–NO bonds both in the ground state and the excited states, whereas the ligands of the equatorial plane show significant influence on the activation barriers along the excitation and decay paths. From the sparse data presently available, the assumption that π -donating equatorial ligands lower the activation barrier for an NO motion, *i.e.*, that they stabilise the transition states even more efficiently than the minima, possibly both in the course of a PLI and a PR event, may be formulated as an entry to future work.

Acknowledgements

Financial support by DFG (WO618/8-1) and BMBF (FKZ 03 × 5510) is gratefully acknowledged (D. S. and T. W.). The authors thank Martina Preiner for contributing to this work during her research course.

Notes and references

‡ K₂[Ru(NO)Cl₂] and [Ru(NO)Cl₂(terpy)]PF₆ were prepared according to literature procedures.^{19,20} [Ru(NO)Cl₂(terpy)]PF₆ (200 mg, 0.344 mmol) was suspended in 0.1 M NaOH (12 mL, 1.2 mmol). Glycolic acid (88 mg, 1.136 mmol) was added and the suspension was heated to 80 °C for 2 h under stirring. After cooling, NaBPh₄ (118 mg, 0.344 mmol) was added and the resulting orange precipitate was filtered off, washed with water (50 mL) and the resulting solid was dried *in vacuo* (210 mg, 0.277 mmol, 80% yield). ESI HR-MS (positive ion, *M* = C₁₇H₁₃N₄O₄Ru): *m/z* calcd: 438.9980, found: 438.9979. ¹³C{¹H} NMR (100.53 MHz, *d*₆-dmsol): δ ppm (the subscripts α and β refer to the glycolate's carboxyl and hydroxyl-bearing carbon atom, respectively) 181.6 (C _{α}), 164.1–162.6 (4C, C_{*ipso*}), 158.8 (terpy), 153.8 (terpy), 151.3 (2C, terpy), 144.4 (terpy), 142.8 (2C, terpy), 135.5 (8C, C_{*ortho*}) 133.0 (terpy), 129.2 (2C, terpy), 126.6 (terpy), 126.4 (2C, terpy), 125.3 (8C, C_{*meta*}), 125.1 (2C, terpy), 121.5 (4C, C_{*para*}), 72.0 (C₈). UV/Vis (dmsol): λ_{\max} nm (ϵ/L mol^{−1} cm^{−1}): 346 (10995). The NMR assignments were confirmed by DFT calculations. Crystals suitable for X-ray crystallography were obtained by dissolving the product in dmsol and slowly evaporating the solvent. A suitable crystal was selected with the aid of a polarising microscope, mounted on the tip of a glass fiber and investigated at 200 K

on a Nonius Kappa CCD diffractometer with graphite-monochromatised Mo K α radiation ($\lambda = 0.71073$ Å). The structure was solved by direct methods (SHELXS-97) and refined by full-matrix least-square calculations on *F*² (SHELXL-97). Anisotropic displacement parameters were refined for all non-hydrogen atoms with the exception of solvent molecules. Crystallographic data of [Ru(NO)(terpy)L]BPh₄·dmsol: C₄₃H₃₀N₄O₅RuS, *M_r* = 835.72 g mol^{−1}, crystal size: 0.51 × 0.09 × 0.08 mm, *T* = 200(2) K, orthorhombic, *Pbca*, *a* = 11.3863(2), *b* = 23.9172(5), *c* = 28.1252(5) Å, *V* = 7659.3(2) Å³, *Z* = 8, ρ = 1.449 g cm^{−3}, μ = 0.516 mm^{−1}, 56 805 observed reflections, 8770 reflections in refinement, 493 parameters, *R*(*F*) = 0.0515, *R_w*(*F*²) = 0.1263, *S* = 1.003, shift/error_{max} = 0.001, max. and min. residual electron density: 0.874 and −0.931 e Å^{−3}. † The infrared spectra were detected with a Nicolet 5700 FTIR spectrometer. The fine powder was mixed with KBr and pressed to a pellet. The KBr pellet was mounted on a copper cold finger using silver paste for good thermal contact. The sample was cooled to 80 K in a liquid nitrogen cryostat. CsI windows allowed the irradiation of the sample with laser light and absorption measurements down to 260 cm^{−1}. The irradiation was performed by the monochromatic light of an argon laser at 457.9 nm, 476.5 nm, 488 nm, or 496.5 nm or a HeCd laser at 442.5 nm for the population of the metastable state MS1. The transfer from MS1 into MS2 was performed with light of a Nd:YAG laser at 1064 nm after MS1 had been previously generated up to saturation with blue-green light. The electronic and structural ground state of the cation of the title compound as well as the MS1 and MS2 in their diamagnetic electronic state were modelled by means of DFT calculations on the B3LYP/SDD/6-31G(d,p) level of theory using the SDD core potential for ruthenium. All stationary points were confirmed by frequency analyses.

- J. H. Enemark and R. D. Feltham, *Coord. Chem. Rev.*, 1974, **13**, 339–406.
- M. J. Rose and P. K. Mascharak, *Coord. Chem. Rev.*, 2008, **252**, 2093–2114.
- P. Gütllich, Y. Garcia and T. Woike, *Coord. Chem. Rev.*, 2001, **219–221**, 839–879.
- P. Coppens, I. Novozhilova and A. Kovalevsky, *Chem. Rev.*, 2002, **102**, 861–884.
- T. E. Bitterwolf, *Coord. Chem. Rev.*, 2006, **250**, 1196–1207.
- K. Karidi, A. Garoufis, A. Tsipis, N. Hadjiliadis, H. d. Dulk and J. Reedijk, *Dalton Trans.*, 2005, 1176–1187.
- D. Schaniel, T. Woike, C. Merschjann and M. Imlau, *Phys. Rev. B: Condens. Matter Mater. Phys.*, 2005, **72**, 195119/1–195119/5.
- D. Schaniel, T. Woike, B. Delley, D. Biner, K. W. Kramer and H.-U. Gudel, *Phys. Chem. Chem. Phys.*, 2007, **9**, 5149–5157.
- D. Schaniel, B. Cormary, I. Malfant, L. Valade, T. Woike, B. Delley, K. W. Kramer and H.-U. Gudel, *Phys. Chem. Chem. Phys.*, 2007, **9**, 3717–3724.
- S. Ferlay, H. W. Schmalle, G. Francese, H. Stoeckli-Evans, M. Imlau, D. Schaniel and T. Woike, *Inorg. Chem.*, 2004, **43**, 3500–3506.
- D. Schaniel and T. Woike, *Phys. Chem. Chem. Phys.*, 2009, **11**, 4391–4395.
- B. Delley, *Z. Kristallogr.*, 2008, **223**, 329–333.
- O. V. Sizova, O. O. Lubimova, V. V. Sizov and N. V. Ivanova, *Z. Kristallogr.*, 2008, **223**, 343–355.
- S. I. Gorelsky, S. C. da Silva, A. B. P. Lever and D. W. Franco, *Inorg. Chim. Acta*, 2000, **300–302**, 698–708.
- S. I. Gorelsky and A. B. P. Lever, *Int. J. Quantum Chem.*, 2000, **80**, 636–645.
- P. Coppens, I. Novozhilova and A. Kovalevsky, *Chem. Rev.*, 2002, **102**, 861–884.
- G. F. Caramori and G. Frenking, *Organometallics*, 2007, **26**, 5815–5825.
- A. Zangl, P. Klüfers, D. Schaniel and T. Woike, *Dalton Trans.*, 2009, 1034–1045.
- J. R. Durig, W. A. McAllister, J. N. Willis and E. E. Mercer, *Spectrochim. Acta*, 1966, **22**, 1091–1100.
- T. Hirano, K. Ueda, M. Mukaida, H. Nagao and T. Oi, *J. Chem. Soc., Dalton Trans.*, 2001, 2341–2345.
- I. N. Levine, *Quantum chemistry*, Prentice Hall, Upper Saddle River, NJ, 5th edn, 2000.